ICIT 2015 The 7th International Conference on Information Technology
doi:10.15849/icit.2015.0107

Enhanced Watermarking Scheme for 3D Mesh Models

Lamiaa Basyoni
College of Computing and Information Technology
Arab Academy of Science and Technology
Cairo, Egypt
lamiaa.basyoni@gmail.com

H. I. Saleh
Radiation Engineering Department
Atomic Energy Authority
Cairo, Egypt
h_i_saleh@hotmail.com

M. B. Abdelhalim
College of Computing and Information Technology
Arab Academy of Science and Technology
Cairo, Egypt
mbakr@ieee.org

***Abstract*— In this paper we present a new non-blind watermarking scheme for 3D graphical objects (meshes). Non-blind watermarking scheme is known to be more secure than blind ones, since the original and watermarked models are needed for extraction. In our scheme we use the model's prominent feature points to divide the model into separate segments, these feature segments are then projected from 3D representation to the 3 main 2D-Planes. The watermark embedding is done in frequency domain of these projections. The experimental results showed the robustness of this scheme against various mesh attacks (mesh simplification, subdivision, smoothing, cropping, etc). This scheme also allows quite large payload to embed. The results of the proposed scheme showed average of 50 percent improvement in robustness against geometry attacks, and up to 70 percent against connectivity attacks.**

Keywords*— *Digital Watermarking, 3D Models, Triangular Mesh, Robust Watermarking.

I. INTRODUCTION

3D mesh models are rapidly growing in the multimedia applications, and are used more and more in many fields, with industrial, medical, and entertainment applications. This increases the need for intellectual property protection and authentication.

Digital watermarking was found to be a very efficient solution for the authentication problems. This technique carefully hides some secret information in the functional part of the cover content. A watermark is a digital code permanently embedded into a cover content [1]. A watermark can be embedded in a variety of cover content types, including images, audio data, video data, and 3D graphical objects.

The 3D graphical objects are the most difficult kind of digital media to design a watermarking framework for, as it has many challenges [2], such as: (1) Low volume of data: the amount of data available to hide the watermark in it is very low as a 3D model consists of a few thousands of vertices unlike the enormous amount of pixels provided in the case of images.(2) No unique representation: an image is represented as a 2D array, while a 3D model can be represented in many different ways. (3) No robust transformation field that can be used for embedding. (4)Attacks may change the geometry and connectivity properties of the mesh. (5)High computational requirements, specially for frequency domain implementation.

Watermarking techniques are generally classified based on the detection method to blind and non-blind techniques. Blind techniques require neither the cover (original model) nor the embedded watermark to extract the watermark, while the non-blind techniques need the cover content in order to complete the extraction process, so that, the possession of the original model becomes part of the proof of ownership[3]. The non-blind watermarking is more robust than the blind watermarking. Both techniques gained a lot of attention

doi:10.15849/icit.2015.0107

recently, many algorithms were developed to provide robust watermarking scheme [4].

In the first category, a recent blind watermarking technique was developed based on multi resolution representation and fuzzy logic. Fuzzy logic approach approximates the best possible gain with an accurate scaling factor so that the watermark remains invisible. The fuzzy input variables are computed for each wavelet coefficient in the 3D model. The output of the fuzzy system is a single value which is a perceptual value for each corresponding wavelet coefficient. Thus, the fuzzy perceptual mask combines all these non-linear variables to build a simple, easy to use HVS (human visual systems) model. Results showed that the system is robust against affine transformations, smoothing, cropping, and noise attacks [5].

Another blind watermarking scheme based on volume moments was introduced by Wang, et al [6]. During watermark embedding, the input mesh is first normalized to a canonical and robust spatial pose by using its global volume moments. Then, the normalized mesh is decomposed into patches and the watermark is embedded through a modified scalar Costa quantization of the zero-order volume moments of some selected candidate patches [6].

In the second category, there is the non-blind watermarking algorithm based on geometrical properties of 3-D polygon mesh introduced by Garg, H., et al [4]. The objective of this algorithm is to process the object to find the less visible area of 3D polygonal mesh. Another non-blind watermarking scheme that was developed by Ryutarou Ohbuchi, et al [7], uses the spectral domain to embed the watermark. The algorithm computes spectra of the mesh by using eigenvalue decomposition of a Laplacian matrix derived only from connectivity of the mesh.

The rest of the paper is structured as follows: section 2 provides an overview of the segmentation operations we apply on the mesh model. Section 3 describes the steps of embedding and extracting the watermark. In Section 4 we illustrate the main features of our implementation. The experimental results are provided in section 5, and a conclusion of the paper is presented in section 6.

II. SEGMENTATION

The first step in our algorithm is to divide the original mesh model into core part, and a number of segments contain its feature points. In this section we describe the used segmentation method based on [8]. The feature points selected are the prominent points of the model. These points reside on the tip of prominent components of the model. For instance, in Fig.1, feature points can be found on the tip of the tongue, horn, and tail. To formally define the vertices on the tips, it should satisfy the following conditions.

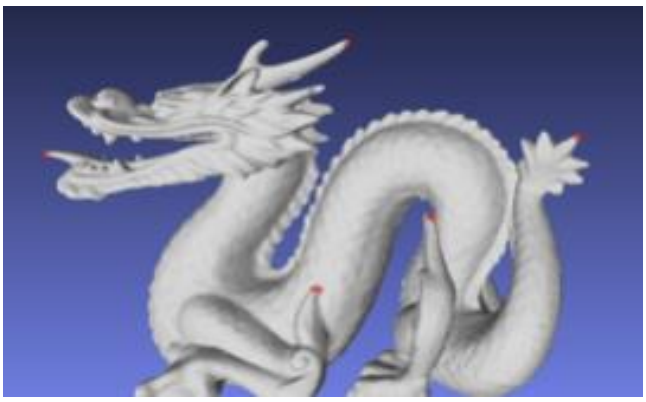

Fig. 1. Prominent Feature Points

∀v ∈ S, let Nv be the set of neighbouring vertices of vertex v. Let GeodDist(vi, vj) be the geodesic distance between vertices vi and vj of mesh S. The local condition that a feature point should satisfy is that ∀vn ∈ Nv.

$$\sum_{v_i \in S} GeodDist(v, v_i) > \sum_{v_i \in S} GeodDist(v_n, v_i) \quad (1)$$

The feature points determined are then used to guide the segmentation. The mesh is segmented into its core component and its prominent components. Each prominent component is defined by one or more of the feature points, while the core components are closer to the center of the mesh model. The segmentation process consists of the following 3 steps:

1) *Spherical Mirroring:*
   Prominent feature points on surface S tend to be extreme in some direction, while vertices of the core component tend to be closer to the center of S, the aim of spherical mirroring is to reverse this situation, and the vertices of the core become external and can be easily extracted.
2) *Core Component Extraction*:
   The convex hull of the mirrored vertices is computed. The vertices that reside on the convex hull, along with the faces they define on S, are considered the initial core component.
3) *Extraction of the other segments*:
   Once the core component is found, the other segments of the mesh are extracted by "subtracting" the core component from the mesh.

A. Segments Projection

The term *projection* refers to any dimension-reduction operation. One way to achieve this is using a scale factor of zero in a certain direction, thus, all points will be projected onto the perpendicular plane (in our 3D case). This type of projection is called Orthographical Projection or Parallel Projection as shown in Fig.2. In our framework, we use parallel projection to convert the feature segments selected of the 3D mesh model into three 2D-arrays, each obtained by projecting against one of the 3 cardinal axes.

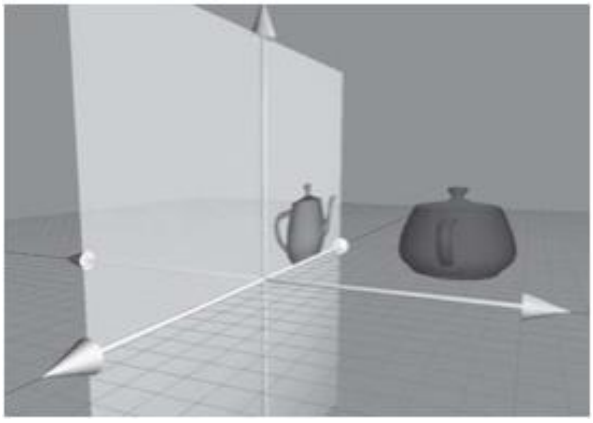

Fig. 2. parallel Projection of a 3D object

doi:10.15849/icit.2015.0107

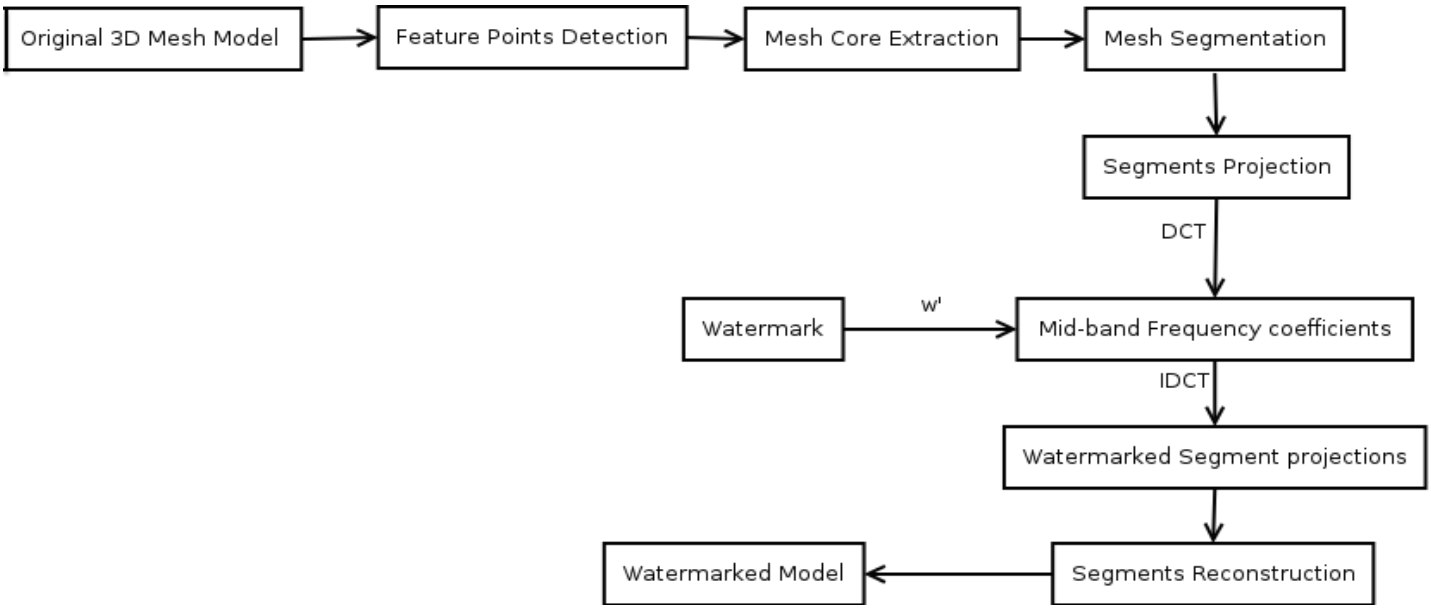

Fig.3. Steps of the watermarking embedding process

To project a 3D model or a segment of it onto a plane, we use a scale value of zero on the perpendicular axis to this plane [8]. The 3D matrices used for projection on the xy, xz, and yz planes are as follows:

$$P_{xy} = \begin{bmatrix} 1 & 0 & 0 \\ 0 & 1 & 0 \\ 0 & 0 & 0 \end{bmatrix}$$

$$P_{xz} = \begin{bmatrix} 1 & 0 & 0 \\ 0 & 0 & 0 \\ 0 & 0 & 1 \end{bmatrix}$$

$$P_{yz} = \begin{bmatrix} 0 & 0 & 0 \\ 0 & 1 & 0 \\ 0 & 0 & 1 \end{bmatrix}$$

III. Watermark Embedding And Detection

A. *Watermark Embedding Process*

The watermark embedding process is based on the segmentation process, and the segments projection explained in the previous section. Fig.3. shows the scheme we use for watermark embedding process. In our scheme we use a sample image as watermark payload. The pixels of the image (with values 0 and 1 only) are embedded in the selected segments defined by the feature points of the model. The watermark image is split into equal blocks of pixels, as shown in Fig.4. Each block is then embedded in a segment of the 3D model.

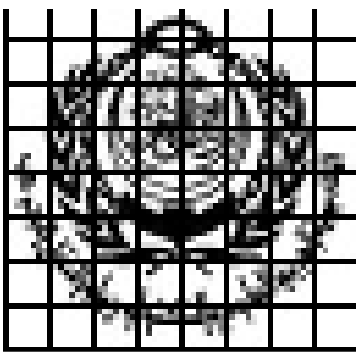

Fig. 4. Watermark Image split into blocks

Dividing the image watermark into blocks and distribute it among the feature segments increase the resistance for attacks like cropping. It has been proved in cases of image, audio, and video watermarking that it is better to embed information in spectral domain rather than in the spatial domain based on [1]. Many of the new researches focus on the use of frequency domain for its robustness compared to other domains [14]. Robustness is a key factor in our algorithm, so we're adopting the DCT (discrete cosine transform)-based watermarking method. DCT is selected for its computational simplicity compared to other transforms such as Discrete Fourier Transform. It also has the ability to pack more information in fewer coefficients. The DCT coefficients are divided into 3 main bands; low frequencies, mid frequencies, and high frequencies, as shown in Figure 5. Embedding in the mid-band coefficients avoid scattering the watermark information to most visual parts of the model i.e. the low frequencies and also it do not overexpose them to removal through noise attacks where high frequency components are targeted.

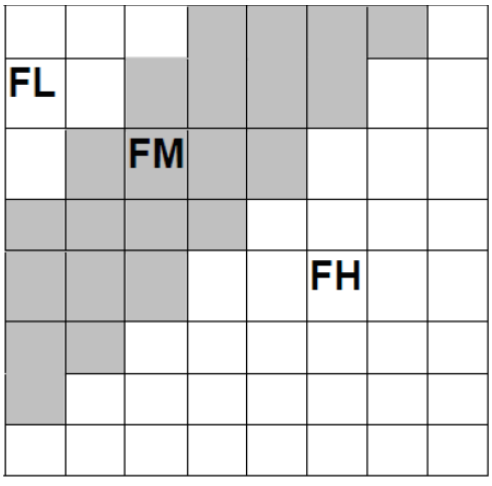

Fig. 5. DCT coefficients for 8*8 block

doi:10.15849/icit.2015.0107

The watermarking process can be described as follows:

- The arrays resulting from the projection of the feature segments are divided into blocks, and DCT is applied on each block
- A number (N) of the mid-band coefficients is selected, where N = 1/4 the width of the watermark image.
- The embedding is then performed in the transform domain; the logo image we use is represented as 0's and 1's. If the pixel value to be embedded is 0, then there will be no changes in the coefficient value: C' = C. Otherwise the coefficient will be changed to C' = C + w. C, where C' is the DCT coefficient after embedding, and w is the watermark ratio, that has a direct effect on the visual quality of the model. Figure 6 shows the effect of the watermark ratio w on the visual quality measured by the Root Mean Square error (RMS) and the bit error rate of the watermark after extraction. At 7% of the coefficient values we reach an acceptable RMS value (according the watermarking benchmark [13]), and the watermark can be fully recovered.
- IDCT (inverse discrete cosine transforms) is then applied to these blocks to generate the watermarked segments projections.
- We then reverse the projection steps to re-create the watermarked segments.
- 3D object reconstruction by combining the core part with the watermarked feature segments.

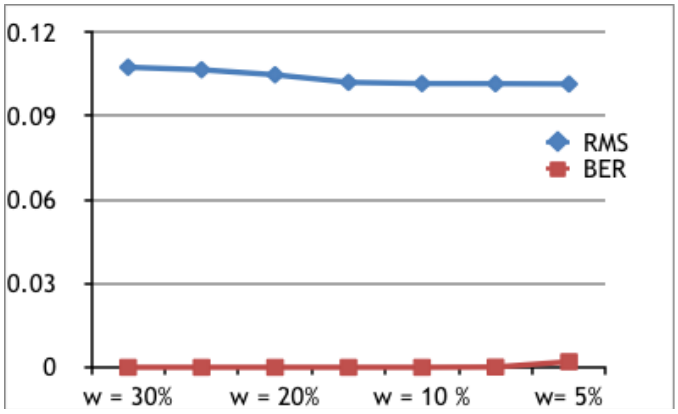

Fig. 6. The effect of different watermark ratios on visual quality and the Bit Error Rate

B. Watermark Extraction Process

Fig.7. shows the block diagram of watermark extraction process. The process has the same steps to create the segments projection, and since we're adopting a non-blind technique, the original segments projections are needed to complete the extraction process. We use the same process, whether the watermarked model is attacked or not.

The array of segments projection generated for both watermarked and original models will be the input for DCT operation. The same range of mid-band coefficients is selected to extract the watermark:

$$W_L = \frac{C_W - C_O}{\beta \cdot C_O} \qquad (2)$$

the watermarking extracting process

Where C_W is the coefficient obtained for the watermarked model, C_O is the original model coefficient, and W_L is the detected value for the corresponding pixel in the logo image, it should have the value of 0 or 1. This way the logo image will be re-constructed. The original image will be compared to the extracted image using the PSNR (peak signal to noise ratio) measure to calculate the efficiency of our watermarking scheme.

IV. Experimental Results

A. *Distortion Evaluation*

The described scheme was applied on different 3D models whose characteristics are listed in Table 1.

Table.1. Characteristics of the 3D models used in experiments.

Object	No. Vertices	No. Faces
Bunny	34835	69666
Dragon	50000	100000
Hand	36619	72958
Rabbit	70658	141312
Venus	100759	201514

The results of applying our scheme on the five objects are shown in Fig.8.

doi:10.15849/icit.2015.0107

The models were selected to provide a diversity of mesh shapes; a shape like the bunny has many rounded faces, where

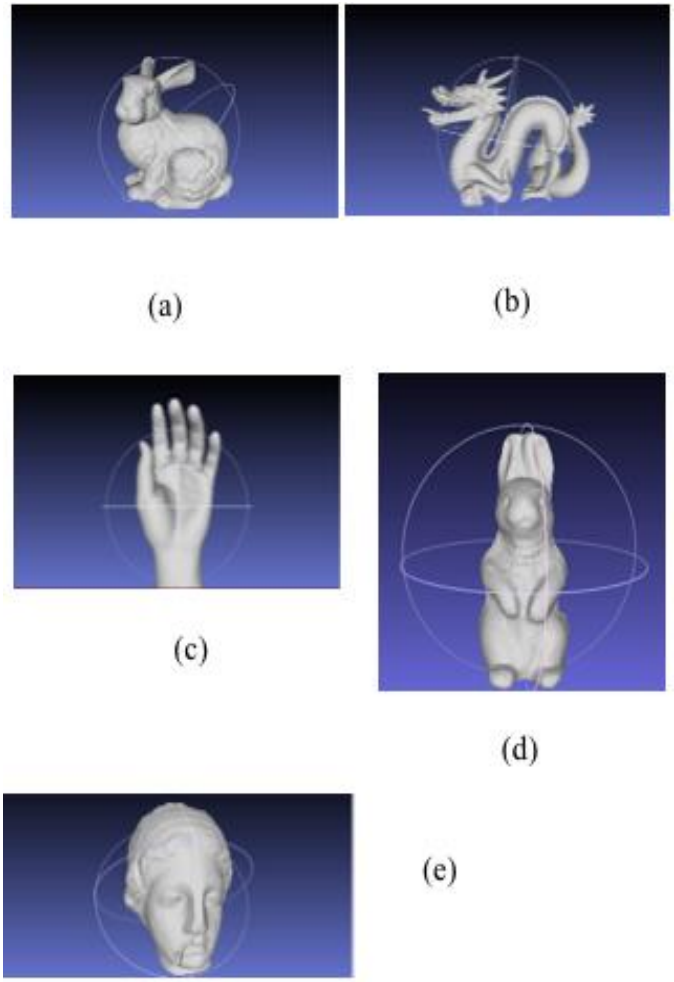

Fig. 8. 3D models used in our experiments: (a) bunny, (b) dragon, (c) hand, (d) rabbit, and (e) venus.

the dragon shape is very complex. There is also an elongated object (the rabbit), and the hand object is quite flat.

The watermark embedding process introduces some distortion to the original cover mesh. This distortion can be measured using many metrics; we are using the root mean square error (RMS) between two 3D-surfaces which is more accurate than other simple vertex-to-vertex distance measures (e.g. PSNR). The RMS is defined in eq.3.

$$d_{RMS}(S,S') = \sqrt{\frac{1}{|S|}\sum_{p\in S} d(p,S')^2} \qquad (3)$$

Where p is a point on surface S, S' is the surface to measure the distance to, |S| is the area of S, and d(p,S`) is the distance between p and S`. The amount of distortion introduced by a watermarking technique is one of the evaluation factors; it's required to present the minimal amount of distortion. The method used to measure the quality of the watermarked models is Metro [10]. Mesh models are usually used in digital entertainment applications, so it has to be assured that the embedding of the watermark will not affect the visual quality of the models. Based on the evaluation criteria defined by the benchmark of 3D models watermarking [11] the induced geometric distortion should be <0.09 with respect to the diagonal of the bounding box. Table.2 shows the baseline evaluation results of the proposed scheme and Wang's algorithm [12], stating the payload size used with every model and the visual effect of it in terms of the perceptual quality measure RMS. The evaluation shows that our scheme is supporting much larger payload, while maintaining the models visual quality. In Table.3 the ratio between payload and RMS is presented to show that our scheme is better by 36% in preserving the visual quality of the 3D Model for large watermarking payloads.

Table.2 Baseline Evaluation Results

	Payload		**RMS(w.r.t. l_{bbd})**	
Model	***Wang's***	***Proposed Scheme***	***Wang's***	***Proposed Scheme***
Venus	75	256	0.0023	0.0027
Bunny	67	144	0.0017	0.0053
Horse	46	64	0.001	0.0014
Dragon	49	256	0.0018	0.0057
Average Values	**59.25**	**180**	**0.0017**	**0.0038**

Table.3 Payload to RMS Ratio

	Wang's	***Proposed Scheme***
Payload/RMS	34852	47368

The visual effects of embedding the watermark in the mesh models are illustrated by zooming in details of the models (Fig.9).

doi:10.15849/icit.2015.0107

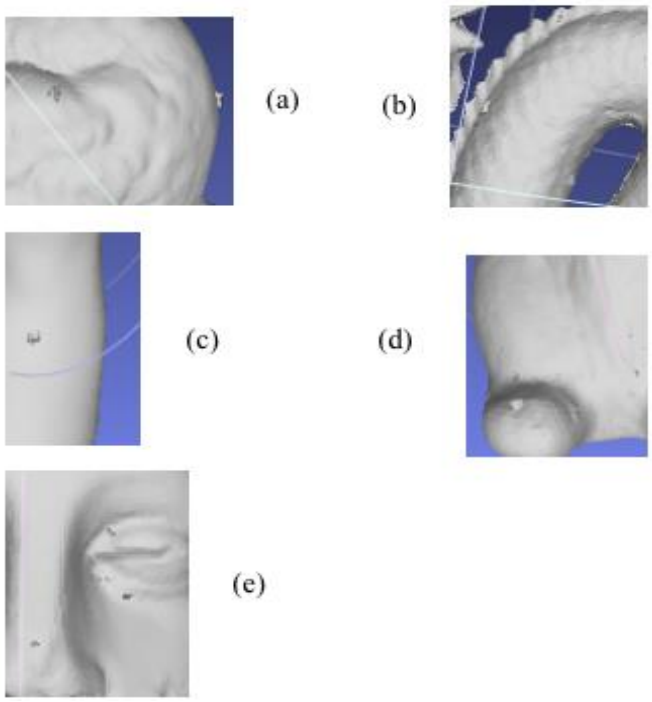

Fig. 9. Zoom-in area of the watermarked models shows the distortion added.

B. Information Embedding Capacity

In our proposed scheme we provide embedding capacity (watermark payload) that varies according to the model size and number of feature point (a logo image of 16x16 pixels, up to 24x24 pixels), which gives the ability to hide a considerably large data..

C. Robustness Evaluation

In this section we present the evaluation of our watermarking scheme against various 3D mesh attacks, in general there are three kind of routine attacks applied on watermarked meshes: *file attacks*, *geometry attacks*, and *connectivity attacks.* In the following we present the results of applying a diversity of these attacks, by measuring the amount of distortion introduced by these attacks on the watermarked model, and the quality of extracted watermark

- Cropping: one of the connectivity attacks in which one part of the watermarked mesh is cut off and lost, we applied this attack on the model where 12% of the mesh vertices were lost as shown in Fig.10 (a).

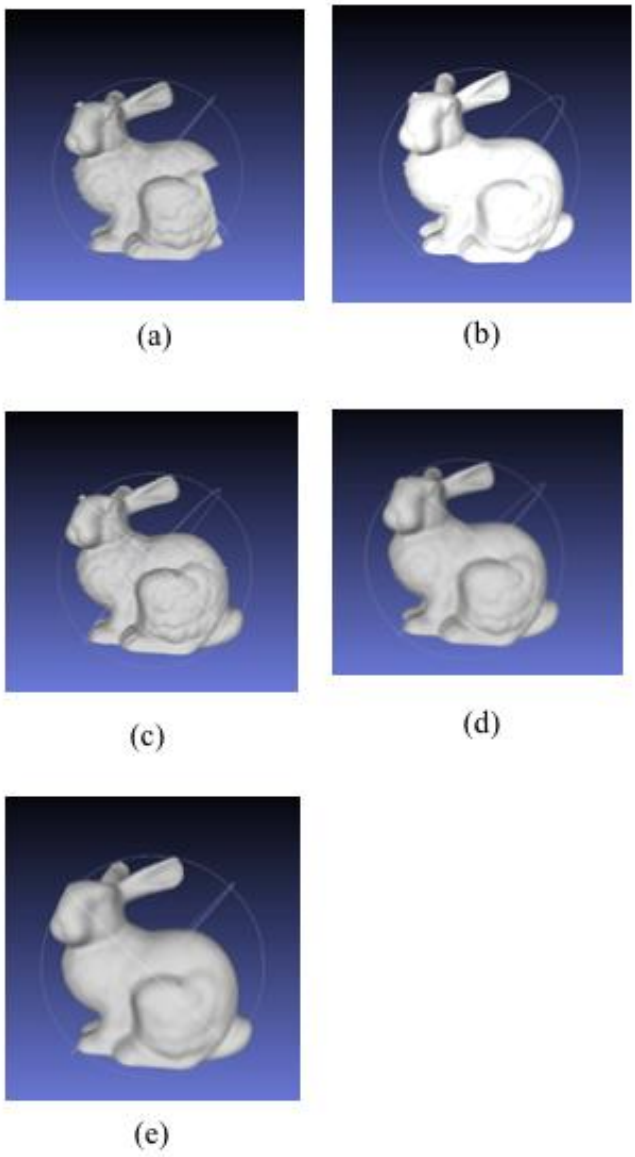

Fig. . The watermarked bunny model after applying 5 different attacks : (a) Cropping, (b) Subdivision using loop scheme, (c) Subdivision using mid-point scheme, (d) Laplacian Smoothing using 3 iteration, (e) Laplacian Smoothing using 10 iterations.

- Subdivision: a connectivity attack in which vertices and edges are added to the mesh to obtain a smoother and higher visual quality version of the model. Two different schemes of subdivision are used: the loop scheme [Fig.10 (b)], and the mid-point scheme [Fig.10. (c)].

doi:10.15849/icit.2015.0107

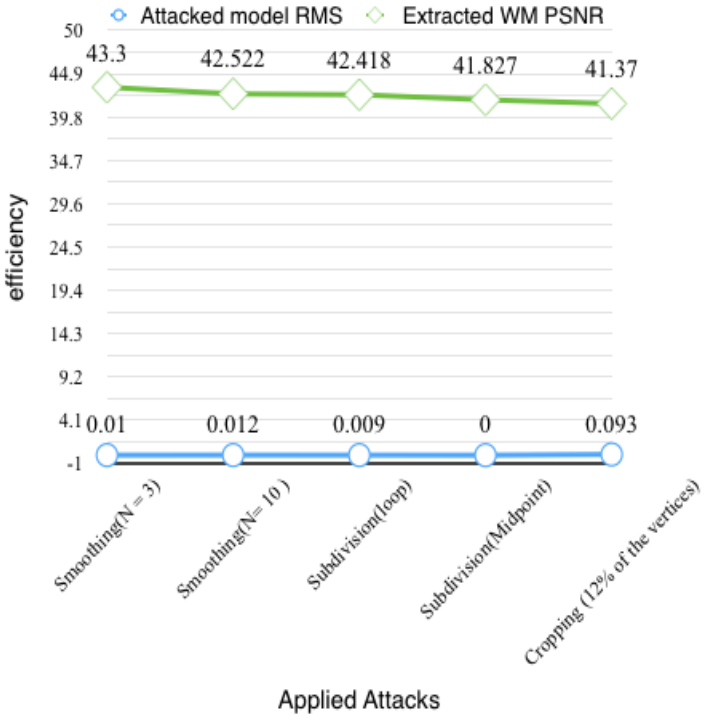

Fig.11. The effects of some attacks on the visual quality of the watermarked model and the efficiency of watermark extraction.

- Smoothing: a geometry attack that's also a common process used to remove the noise generated during the mesh generation process. Referring to the benchmark we adopt [12] we applied Laplacian smoothing with different number of iterations [N =3, N= 10], its effect is shown in Fig.10 (d) and (e) respectively. Applying these attacks on the watermarked mesh introduces different amount of distortion, and affects the hidden data in its own way. In Fig.11, we plot the effect of these attacks on the bunny model. The PSNR measures the quality of the watermark image restored after applying the attacks, the results show that the watermark is efficiently extracted from the attacked model.

V. Results Comparison

In order to show the robustness of our scheme, it is compared to other schemes. Referring to the benchmark we used for evaluating the embedding effect on the models, it presents 2 different algorithms to compare with, the work of Wang et al. [11] that is based on modification of the mesh local volume moments, and the work of Cho et al. [12] that is based on modification of the mean value of the histogram of vertex norms.

Table.4 Robustness Comparison between the 3 methods

Attacks	***Chos's BER***	***Wang's BER***	***Proposed Scheme BER***
Similarity Transformation	0.0	0.0	0.0
Smoothing N = 5	**0.01**	**0.0**	**0.013**
Smoothing N = 10	0.23	0.01	0.015
Smoothing N = 30	0.38	0.07	0.02
Smoothing N = 50	0.45	0.14	0.02
Average Geometry Attacks	**0.214**	**0.044**	**0.014**
Subdivision Midpoint	**0.04**	**0.0**	**0.02**
Subdivision	0.14	0.0	0.04
Subdivision Loop	0.16	0.0	0.045
Simplification E = 10	0.01	0.0	0.02
Simplification E = 30	**0.05**	**0.0**	**0.019**
Simplification E = 50	0.18	0.0	0.025
Simplification E = 70	0.33	0.0	0.029
Simplification E = 90	0.23	0.01	0.031
Cropping 10%	**0.5**	**0.51**	**0.012**
Cropping 30%	0.53	0.49	0.014
Cropping 50%	0.51	0.49	0.013
Average Connectivity Attacks	**0.243**	**0.136**	**0.024**

The benchmark limits the used payload to be around 70 bits in order to conduct a meaningful comparison, so we are reducing the size of our embedded watermark logo to an 8x8 image, which gives us 64 bits to be embedded. The perceptual protocol defined by the benchmark is applied, and the Bit Error Rate (BER) is calculated as a measure of robustness. Table 4 shows a comparison of the BER computed after applying a number of attacks on Venus model. Embedding the watermark in the middle frequency band does not expose it to removal by operation targeting the higher frequencies such as smoothing, and it can be noted that our scheme gives a remarkable robustness against this kind of attacks even at large number of iterations. The embedding of the watermark is also scattered between many feature segments that are not necessary interconnected, that makes it more robust against faces removing attacks, such as cropping.

doi:10.15849/icit.2015.0107

CONCLUSION

In this paper, we proposed a new non-blind, frequency domain watermarking scheme that is based on mesh segmentation. The proposed scheme compared to other methods shows a better robustness against both geometry and connectivity attacks. The scheme also preserves the visual quality of the 3D mesh models. A considerably large payload is also supported, which allows hiding of large sum of information, and this one of the most critical issues in 3D models watermarking.

REFERENCES

[1] F. Yu, Three-dimensional model analysis and processing. 1st, ed. Heidelberg: Zhejiang University Press, 2007.

[2] Y. Zhi-qiang, H. H. S. Ip, and L. F. Kowk, 'Robust watermarking of 3D polygonal models based on vertex scrambling', Proceedings Computer Graphics International 2003, pp. 254 - 257. 2003.

[3] S. W. Foo, 'Non-blind audio-watermarking using compression-expansion of signals', APCCAS 2008 - 2008 IEEE Asia Pacific Conference on Circuits and Systems, Jan. 2008.

[4] H. Garg, S. Agrawal, and G. Varshneya, 'A non-blind image based watermarking for 3-D polygonal mesh using its geometrical properties', 2013 Sixth International Conference on Contemporary Computing (IC3), pp. 313 - 318. 2013.

[5] S. Tamane, 'Blind 3D Model Watermarking based on Multi-Resolution Representation and Fuzzy Logic', International Journal of Computer Science and Information Technology, vol. 4, no. 1, pp. 117–126, 2012.

[6] K. Wang, G. Lavoué, F. Denis, and A. Baskurt, 'Robust and blind mesh watermarking based on volume moments', Computers & Graphics, vol. 35, no. 1, pp. 1–19, Jan. 2011.

[7] R. Ohbuchi, S. Takahashi, T. Miyazawa, and A. Mukaiyama, "Watermarking 3D polygonal meshes in the mesh spectral domain," in Proc. of Graphics Interface, Ottawa, Canada, pp. 9–17. 2001

[8] S. Katz, G. Leifman, and A. Tal, 'Mesh segmentation using feature point and core extraction', The Visual Computer, vol. 21, no. 8–10, pp. 649–658, Jan. 2005.

[9] F. Dunn, I. Parberry, "3D Math Premier for Graphics and Game Development", 1st, ed. Wordwar Publishing, Inc. 2002.

[10] Cignoni, Rocchini, and Scopigno, 'Metro: Measuring Error on Simplified Surfaces', Computer Graphics Forum, vol. 17, no. 2, pp. 167–174, Jan. 1998.

[11] K. Wang, G. Lavoué, F. Denis, A. Baskurt, and X. He, 'A Benchmark for 3D Mesh Watermarking', 2010 Shape Modeling International Conference, pp. 231 - 235. 2010.

[12] K. Wang, G. Lavou´e, F. Denis, and A. Baskurt, "Robust and blind watermarking of polygonal meshes based on volume moments," Journal of Computers and Graphics, vol. 35, pp. 1-19 , 2011 .

[13] J. W. Cho, R. Prost, and H. Y. Jung, "An oblivious watermarking for 3D polygonal meshes using distribution of vertex norms", IEEE Trans. on Signal Process., vol. 55, no. 1, pp. 142-155, 2007.

[14] R. K. Megalingam, M. M. Nair, R. Srikumar, V. K. Balasubramanian, and V. S. V. Sarma, 'A Comparative Study on Performance of Novel, Robust Spatial Domain Digital Image Watermarking with DCT Based Watermarking', International Journal of Computer Theory and Engineering, pp. 647–653, Jan. 2010.